Quantitative Determination of Conformer Populations: Assessment of Specific Rotation, Vibrational Absorption, and Vibrational Circular Dichroism in Substituted Butynes

Jiangtao He, Ana Petrovich, and Prasad L. Polavarapu*

Department of Chemistry, Vanderbilt University, Nashville, Tennessee 37235

Received: July 22, 2003; In Final Form: January 7, 2004

To evaluate the quantitative agreement between the observed and predicted properties of specific rotation, vibrational absorption, and vibrational circular dichroism (VCD), (+)-3-chloro-1-butyne, which is one of the smallest single conformer chiral molecules, has been synthesized for the first time and its intrinsic rotation (specific rotation at infinite dilution), vibrational absorption, and VCD have been measured. These properties have also been predicted using density functional theory (DFT) and large basis sets, namely aug-cc-pVDZ, 6-311++G(2d,2p), and aug-cc-pVTZ. Using these experimental and predicted properties, the absolute configuration of (+)-3-chloro-1-butyne is established as (*R*). The observed intrinsic rotation and predicted specific rotation are observed to be in excellent quantitative agreement. The predicted vibrational absorption and VCD spectra are in good qualitative agreement with the corresponding observed spectra; however, the root-mean-square percent differences in integrated intensities are ∼20%−30%. The conformer populations of (−)-3-butyn-2-ol in CCl_4 have then been analyzed using experimental intrinsic rotation, vibrational absorption, and VCD; the corresponding predicted properties were also obtained, using DFT and large basis sets, as for 3-chloro-1-butyne. All three properties indicate that (−)-3-butyn-2-ol exists predominantly in two different conformations in dilute CCl_4 solutions. Populations of these conformers determined from the three methods are in reasonable agreement. However, the errors in populations determined from vibrational absorption and VCD are fairly large, which indicates the need for better quantitative accuracy in the predicted vibrational absorption and VCD intensities.

Introduction

The determination of stable conformers, and of their populations, for a given molecule in the solution phase is a challenging task in many cases. Although microwave spectra or electron diffraction methods yield such information for favorable gas-phase molecules, unique methods for determining this information in the solution phase are difficult to find. Nuclear magnetic resonance (NMR) has been the method of choice for obtaining this information; however, the slow time scale of NMR phenomenon permits the determination of only the average conformation in many cases (3-butyn-2-ol, for example).

Because vibrational spectroscopy is uniquely sensitive to molecular structure—and, hence, to molecular conformation—and vibrational transitions occur on a faster time scale, vibrational spectroscopy, in principle, should be capable of providing the individual conformer populations. During the earlier decades, when ab initio methods were neither practical nor fully developed, the interpretation of vibrational spectral intensities was performed in a semiempirical and qualitative manner. As a result, not much reliance was placed on vibrational spectroscopic methods for determining the conformer populations quantitatively. The recent availability of density functional theory (DFT) methods[1] has led to improved predictions of vibrational spectra, in particular, infrared vibrational absorption (VA) and vibrational circular dichroism (VCD). This capability enhances the utility of VA and VCD for determining the conformer populations. Although numerous VA and VCD studies have been reported in the literature, most studies have focused[2] on qualitative "eyeballing" of the experimental and predicted spectra, with an emphasis on determining the absolute configuration. Although some efforts have been made to determine the conformer populations[3,4] from VA and/or VCD, error limits or uncertainties that are involved in the resulting conformer populations have not been established or analyzed to date.

As reported recently, the variations in specific rotation, as a function of temperature[5] or solvent,[6] can also be used to determine the conformer populations. Specific rotation is an age-old technique that has experienced a renaissance in the past few years, following the first prediction[7] of specific rotation using ab initio methods. Recent implementation of DFT for predicting[8] specific rotation has led to accurate predictions of specific rotation.[9] The specific rotations measured in the gas phase[10] are ideal for comparison with predictions on isolated molecules; however, such measurements require special instrumentation and are not routine. Because the condensed-phase experimental specific rotations (often reported for neat liquids or in some convenient solvent at some convenient concentration) can be influenced by solute−solute interactions, a quantitative comparison of predicted and condensed-phase experimental specific rotations may not be reliable. This drawback can be alleviated with the measurement of intrinsic rotation (specific rotation in the limit of zero concentration),[6] which is devoid of solute−solute interactions. Intrinsic rotation may still be influenced by the solvent (because of solute−solvent interactions); however, such solvent influence can be established by measuring the

* Author to whom correspondence should be addressed. E-mail: Prasad.L.Polavarapu@vanderbilt.edu.

10.1021/jp030889g CCC: $27.50
Published on Web 02/10/2004

intrinsic rotation in different solvents. The combined use of experimental intrinsic rotations and predicted specific rotations is one approach to determine the conformer populations as described in this manuscript.

The purpose of this paper is to evaluate the limits of reliability of specific rotation, VA, and VCD for determining the conformer populations. For this purpose, we have synthesized (+)-3-chloro-1-butyne [HCCC(Cl)(CH_3)H], which is one of the simplest single conformer molecules, and investigated its experimental intrinsic rotation (in carbon tetrachloride (CCl_4) and methanol (CH_3OH) solvents) and its VA and VCD (in CCl_4 solvent). DFT predictions of specific rotation, VA, and VCD of (+)-3-chloro-1-butyne were also obtained using large basis sets, namely, aug-cc-pVDZ, 6-311++G(2d,2p), and aug-cc-pVTZ. A comparison of these observed and predicted quantities provided the limits of quantitative reliability in regard to the use of these methods. We then applied these methods for determining the conformer populations of (−)-3-butyn-2-ol [HCCC(OH)(CH_3)H] in dilute solutions.

Methods

Racemic 3-chloro-1-butyne has been synthesized[11] previously, but individual enantiomers of 3-chloro-1-butyne have not been reported previously, to our knowledge. Following the literature procedure[11a] for racemic 3-choloro-1-butyne, (+)-3-chloro-1-butyne was synthesized from (*S*)-(−)-3-butyn-2-ol via reaction with 1-chloro-*N*,*N*,2-trimethyl-1-propenylamine. The product was purified by distillation. The amount of CH_2Cl_2 impurity was minimized by collecting the distilled product at 68−72 °C. The final product was characterized using NMR. (^{1}H NMR ($CDCl_3$): δ 1.76 (d, 3H, CH_3, $J = 7$ Hz), 2.59 (d, 1H, C≡CH, $J = 2$ Hz), 4.62 (dq, 1H, CHCl, $J = 7$ and 2 Hz).) The electronic circular dichroism spectrum of (+)-3-chloro-1-butyne (0.5 mM in cyclohexane) exhibited one positive band at 192 nm. The enantiomeric purity of (+)-3-chloro-1-butyne was determined as 100% using a chiral gas chromatography (GC) column (Chiraldex G-TA, 20 m × 0.25 mm, Astec, Inc.) with a column temperature of 33 °C, helium as the carrier gas (at 10 psi), and a flame ionization detection (FID) method. Only one GC peak was observed for (+)-3-chloro-1-butyne, whereas two peaks were observed for racemic 3-chloro-1-butyne.

Optical rotation, as a function of concentration, was measured on either an Autopol III (for (−)-3-butyn-2-ol)) or Autopol IV (for (+)-3-chloro-1-butyne) polarimeter, using a 0.5-dm cell. For (−)-3-butyn-2-ol, the following procedure[6] was used. To minimize the errors in concentration/optical rotation, the concentrations were generally chosen to give an observed rotation of ∼0.01° or greater, and the weights of the samples were chosen to be appropriate for 5- or 10-mL solutions. The weight of an empty volumetric flask and the weight of flask with solute were each measured five different times (by removing the flask from, and reinserting the flask into, the balance compartment) to avoid accidental mistakes in the weights. The volumetric flasks were filled with the appropriate solvent, as carefully as humanly possible, up to the mark. This solution was then transferred to a 0.5-dm cell and optical rotation was measured five different times (by removing the cell from, and reinserting the cell into, the sample compartment), to check for consistency. The averages of these measurements were used to calculate the specific rotation. This procedure ensured that no unusual data scatter was present in the measurements. The concentration ranges studied were 0.06−0.33 M in CCl_4 and 0.06−0.29 M in CH_3OH. For (+)-3-chloro-1-butyne, because of the limited amount of sample, we did not follow the procedure used for (−)-3-butyn-2-ol. Instead, solutions were prepared by successive dilution. The concentration ranges studied were 0.01−0.18 M in CCl_4 and 0.02−0.13 M in CH_3OH.

When the observed rotation α varies linearly with concentration (because $\alpha = Ac$, where c is the concentration of optically active substance in solution and A is a proportionality constant), the specific rotation will be a constant (independent of concentration). Nonlinear variation of the observed rotation α with concentration may indicate the influence of solute−solute interactions. If the observed rotation α follows the quadratic equation $\alpha = A_2c^2 + B_2c$, then the specific rotation follows the equation $[\alpha] = A_1c + B_1$. As c tends to zero, the observed rotation α should always approach zero in achiral solvents, and, hence, the plot of α vs c data should be forced to go through the origin. However, specific rotation $[\alpha]$ has a finite value at zero concentration; the constant B_1 in the equation $[\alpha] = A_1c + B_1$ represents the specific rotation at infinite dilution, which is called *intrinsic rotation*,[6,12] and is designated as $[\alpha]_{c=0}$ or $\{\alpha\}$. The linear relation $[\alpha] = A_1c + B_1$ may not apply in all situations; in some cases, $[\alpha]$ may follow quadratic, cubic, or some other complicated relation, in which case the experimental specific rotations are fit to an appropriate model equation. These equations are given in the figure legends. Plots of both α vs c and $[\alpha]$ vs c were prepared. In the normal least-squares fitting procedure, it is a common practice to assume that all the errors are in the y-values. Although this type of fitting is appropriate for α vs c data, weighted least-squares fitting is needed for fitting the $[\alpha]$ vs c data. When these precautions are taken, the intrinsic rotation that is determined from the plot of α vs c will be the same as that obtained from the plot of $[\alpha]$ vs c.

VA and VCD spectra usually contain numerous vibrational bands. In the past, VA and VCD predictions were evaluated[13] against the corresponding experimental observations, by preparing the plots of predicted-versus-experimental integrated band intensities. However, these plots do not provide a quantitative estimate of the agreement/differences. Here, we present, what is believed to be, the first quantitative approach to evaluate VA and VCD intensities. For a single conformer molecule, the agreement between the experimental and predicted intensities can be quantified using the percent difference (PD) and the root-mean-square percent (RMSP) difference:

$$\mathrm{PD} = \left(\frac{P_i - E_i}{E_i}\right) \times 100 \tag{1}$$

where E_i is the observed intensity and P_i is the predicted intensity for band i, and

$$\mathrm{RMSP} = \sqrt{\sum_{i=1}^{m} \frac{[100(P_i - E_i)/E_i]^2}{m}} \tag{2}$$

where the summation runs over m bands of the molecule investigated. For molecules that exist in two or more conformations, the experimental intensities of these bands, in conjunction with predicted intensities for individual conformers, can be used to determine the conformer populations as follows. If the experimental band intensities are represented by a column vector $\{E\}$ and the predicted band intensities for different conformers are represented by a rectangular matrix $\boldsymbol{P}$, then the fractional

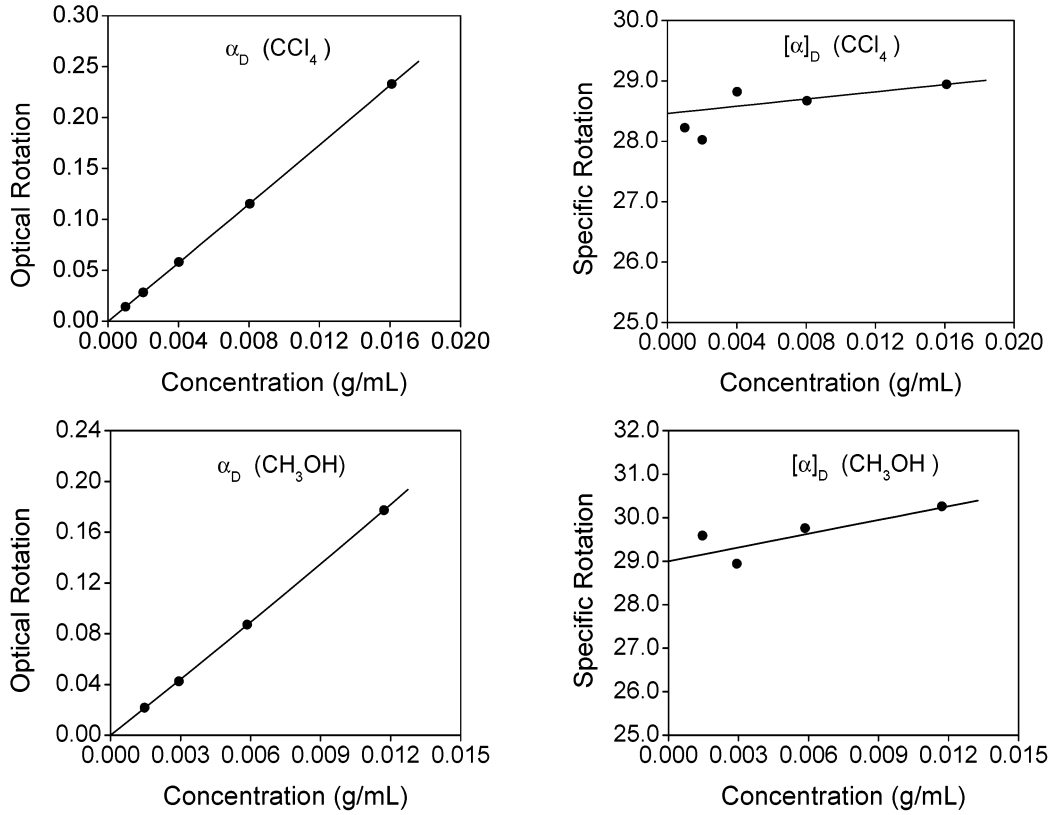

Figure 1. Optical rotation (α_D) and specific rotation ($[\alpha]_D$) of (+)-3-chloro-1-butyne, as a function of concentration in CCl_4 and CH_3OH solutions. In CCl_4, a plot of α_D versus concentration was fit to $\alpha_D = 15.1c^2 + 14.2c$; a plot of $[\alpha]_D$ versus concentration was fit to $[\alpha]_D = 30.0c + 28.4$. In CH_3OH, a plot of α_D versus concentration was fit to $\alpha_D = 52.6c^2 + 14.5c$ and a plot of $[\alpha]_D$ versus concentration was fit to $[\alpha]_D = 105.2c + 29.0$. Fitting of the specific rotation versus concentration required the weighted least-squares method.

populations of conformers, represented by a column vector $\{X\}$, are related to $\{E\}$ and $\boldsymbol{P}$ by eq 3a:

$$\begin{bmatrix} E_1 \\ E_2 \\ E_3 \\ - \\ - \\ - \\ E_m \end{bmatrix} = \begin{bmatrix} P_{1,1} & P_{1,2} & - & P_{1,N} \\ P_{2,1} & P_{2,2} & - & P_{2,N} \\ P_{3,1} & P_{3,2} & - & P_{3,N} \\ - & - & - & - \\ - & - & - & - \\ - & - & - & - \\ P_{m,1} & P_{m,2} & - & P_{m,N} \end{bmatrix} \begin{bmatrix} X_1 \\ X_2 \\ - \\ X_N \end{bmatrix} \tag{3a}$$

In other words, the experimental intensity E_i for band i is expressed as

$$E_i = \sum_{j=1}^{N} P_{ij} X_j \qquad (\text{for } i = 1, 2, \ldots m) \tag{3b}$$

where P_{ij} is the predicted intensity for band i of the jth conformer. Usually, the number of vibrational bands (m) is much greater than the number of conformations (N), so the column vector of fractional populations $\{X\}$ can be determined by regression methods, with the constraints that the sum of the fractional populations of conformers is 1 and fractional populations cannot be negative. That is,

$$\sum_{j=1}^{N} X_j = 1 \tag{4a}$$

and

$$X_j \geq 0 \tag{4b}$$

The experimental VA and VCD spectra were measured on a commercial instrument (Chiral*ir*). The integrated areas of the bands in the experimental spectra were obtained by fitting ($R^2 = 0.99$) the experimental bands to Lorentzian band shapes using the PeakFit program.[14] The experimental band intensities were expressed[15] as dipole strengths (D_i) in VA spectra and as rotational strengths (R_i) in VCD spectra, as follows:

$$D_i = \frac{0.92 \times 10^{-38}}{\nu_0} \int \epsilon(\nu)\, \mathrm{d}\nu \tag{5}$$

$$R_i = \frac{0.23 \times 10^{-38}}{\nu_0} \int \Delta\epsilon(\nu)\, \mathrm{d}\nu \tag{6}$$

where $\epsilon(\nu)$ is the molar absorptivity (in L mol^{-1} cm^{-1}) at frequency ν (in cm^{-1}) and ν_0 is the band center. Vibrational band positions (frequencies) are not needed to use eqs 1−3. However, the predicted counterparts of the experimental bands must be identified and correlated one by one. A commercial program (DataFit)[16] was used to determine the fractional populations, using eqs 3 and 4.

All specific-rotation calculations were performed using a developmental version of the DALTON program.[17] For density functional predictions, a B3LYP density functional that was available in this DALTON program was used. The basis sets used with DALTON were either available in the program library or were obtained from the EMSL library.[18] All specific-rotation calculations reported here were based on gauge-including atomic orbitals (GIAOs, which are also called London orbitals) and the dynamic method.[19] Geometry optimizations and VCD calculations were undertaken with the Gaussian 98 program.[20] The solvent influence on optimized geometries, vibrational

TABLE 1: B3LYP Predicted Specific Rotation ($[\alpha]_D$) of (*R*)-3-Chloro-1-butyne and Experimental Intrinsic Rotation ($\{\alpha\}_D$) of (+)-3-Chloro-1-butyne

method	value
Predicted Specific Rotation, $[\alpha]_D$[a]	
6-31G*	26.8
aug-cc-pVDZ	32.8
6-311++G(2d,2p)	28.3
aug-cc-pVTZ	28.6
average[b]	30 ± 2
Experimental Intrinsic Rotation,[c] $\{\alpha\}_D$	
CCl_4	28.4 ± 0.2
CH_3OH	29.0 ± 0.3

[a] The Gibbs energies of 3-chlorobutyne at the 6-31G*, aug-cc-pVDZ, 6-311++G(2d,2p), and aug-cc-pVTZ levels of theory are −615.512457, −615.556092, −615.598301, and −615.615345 hartrees, respectively. [b] The average value is the average of three large basis-set (aug-cc-pVDZ, 6-311++G(2d,2p), and aug-cc-pVTZ) calculations. [c] Intrinsic rotation (specific rotation in the limit of zero concentration of solute), as derived from a plot of optical rotation versus concentration (see Figure 1).

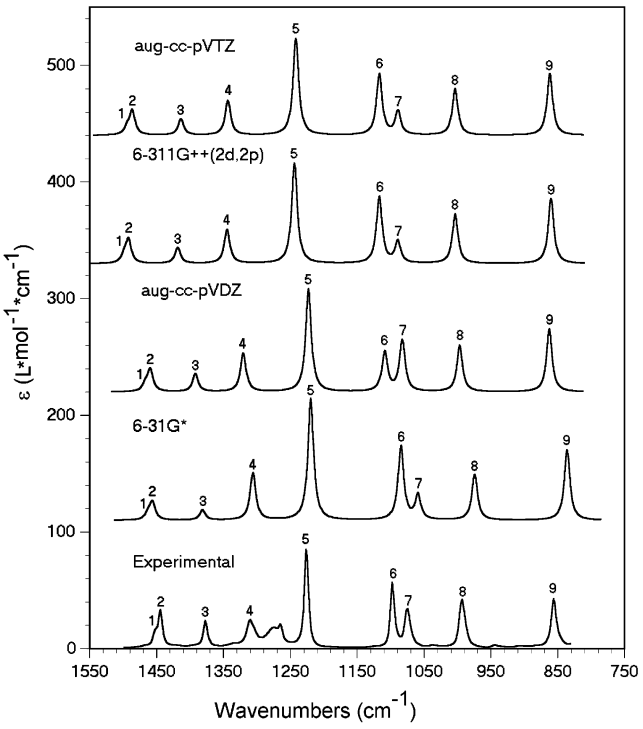

Figure 2. Comparison of experimental absorption spectra of 3-chloro-1-butyne (0.182 M in CCl_4, path length of 300 μm) with the predicted absorption spectra, using different basis sets. The 6-31G* frequencies were scaled by 0.9613, and a bandwidth of 5 cm^{-1} was used in the spectral simulation. Two small absorption bands that are observed in the experimental spectrum at ~1270 cm^{-1} are due to a CH_2Cl_2 impurity.

frequencies, and intensities was investigated with a polarizable continuum model (PCM) that was incorporated in the Gaussian 03 program.

Results and Discussion

(+)-3-Chloro-1-butyne. The concentration dependence of both optical rotation and specific rotation are displayed in Figure 1. The intrinsic rotations derived from these data are 28.4 ± 0.2 in CCl_4 and 29.0 ± 0.3 in CH_3OH solvent. The polarization effect of solvent on the observed intrinsic rotation is quite small, as would be expected for a single conformer molecule without any hydrogen-bonding capability. The specific rotation predicted

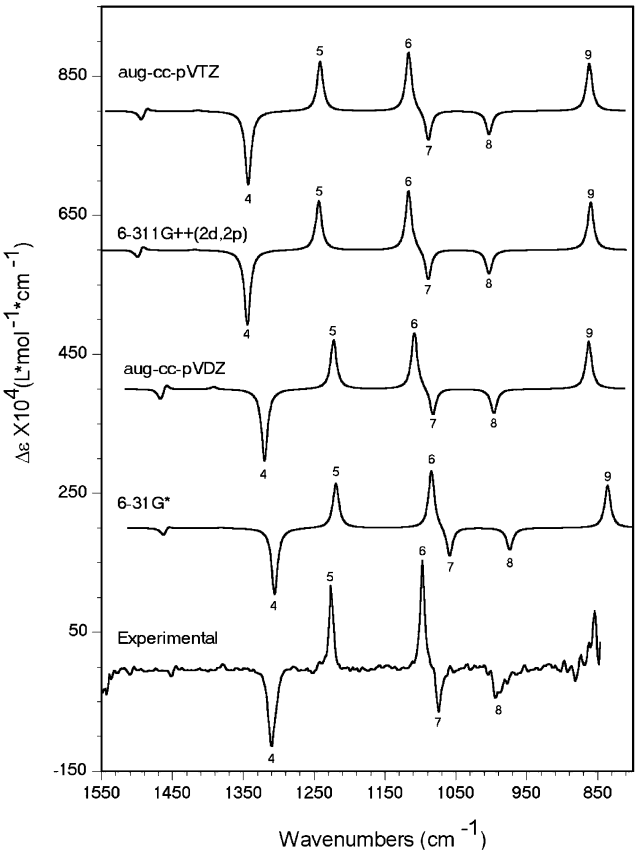

Figure 3. Comparison of experimental vibrational circular dichroism (VCD) spectra of (+)-3-chloro-1-butyne (0.182 M in CCl_4, path length of 300 μm) with the predicted VCD spectra of (*R*)-3-chloro-1-butyne, using different basis sets. The 6-31G* frequencies were scaled by 0.9613, and a bandwidth of 5 cm^{-1} was used in the spectral simulation.

for (*R*)-3-chloro-1-butyne with the B3LYP functional and a small 6-31G* basis set is 26.8, whereas those with large basis sets (aug-cc-pVDZ, 6-311++G(2d,2p), and aug-cc-pVTZ) are 32.8, 28.3, and 28.6, respectively, as summarized in Table 1. The average value of the three large basis-set predictions is 30, which differs from the experimental value in CCl_4 by 7% and from that in CH_3OH by 3.5%. However, because the uncertainty in the predicted average from the three large basis-set calculations is ±2, it can be concluded that the experimental intrinsic rotation is within the uncertainty associated with the three large basis-set predictions.

The VA and VCD spectra predicted for (*R*)-3-chloro-1-butyne using the B3LYP functional and a smaller 6-31G* basis set and three larger basis sets (aug-cc-pVDZ, 6-311++G(2d,2p), and aug-cc-pVTZ) are shown in Figures 2 and 3. The vibrational bands of 3-chloro-1-butyne are well-separated from each other (except for bands 1 and 2), so there is minimal overlap between the bands, which makes it an ideal candidate to quantify the agreement between the experimental and theoretical band intensities. In Figures 2 and 3, one can notice an excellent qualitative agreement between the predicted and experimental spectra. The qualitative "eyeballing" comparison between the simulated and observed VCD spectra clearly confirms the absolute configuration of (+)-3-chloro-1-butyne as (*R*). To evaluate the agreement between the predicted and observed band intensities, the plots of experimental-versus-predicted dipole strengths and rotational strengths are shown in Figure 4. Here, the predicted quantities in B3LYP/aug-cc-pVDZ calculation are used for illustrative purposes. As noted previously, it is difficult to quantify the agreement between experimental observations

TABLE 2: Frequencies (ν_i), Dipole Strengths (D_i), and Rotational Strengths (R_i) for (*R*)-3-Chloro-1-butyne[a]

band number	B3LYP 6-31G*			B3LYP aug-cc-pVDZ			B3LYP 6-311++G(2d,2p)			B3LYP aug-cc-pVTZ			Experiment		
	ν_i	D_i	R_i	ν_i	D_i	R_i	ν_i	D_i	R_i	ν_i	D_i	R_i	ν_i	D_i	R_i
1	1522	5.0	−2.7	1467	6.0	−4.2	1499	5.4	−3.1	1494	5.5	−3.4	1452	8.1	
2	1515	14.3	1.1	1459	18.6	2.4	1492	19.9	2.1	1496	20.1	1.9	1444	24.1	
3	1437	8.7	0.3	1392	16.3	1.0	1418	13.9	0.4	1414	14.1	0.4	1377	18.8	
4	1358	43.1	−26.4	1320	36.3	−28.5	1344	31.4	−29.1	1343	32.0	−28.5	1310	37.0	−37.8
5	1268	118.7	19.2	1223	104.2	20.9	1244	99.7	20.6	1242	96.4	20.9	1226	69.8	20.6
6	1128	81.3	28.1	1109	44.3	27.2	1117	74.4	28.2	1117	67.9	27.9	1097	48.8	34.3
7	1101	27.5	−14.6	1083	58.0	−13.2	1089	24.9	−14.9	1089	26.7	−14.7	1075	42.9	−18.4
8	1013	55.9	−11.7	997	57.6	−13.0	1003	61.2	−12.2	1004	57.7	−12.1	993	58.7	−17.5
9	870	100.3	26.4	863	90.7	28.7	860	93.9	29.1	862	89.8	28.9	856	66.6	

[a] Frequencies are given in units of cm^{-1}, dipole strengths are given in units of 10^{-40} esu^2 cm^2, and rotational strengths are given in units of 10^{-44} esu^2 cm^2.

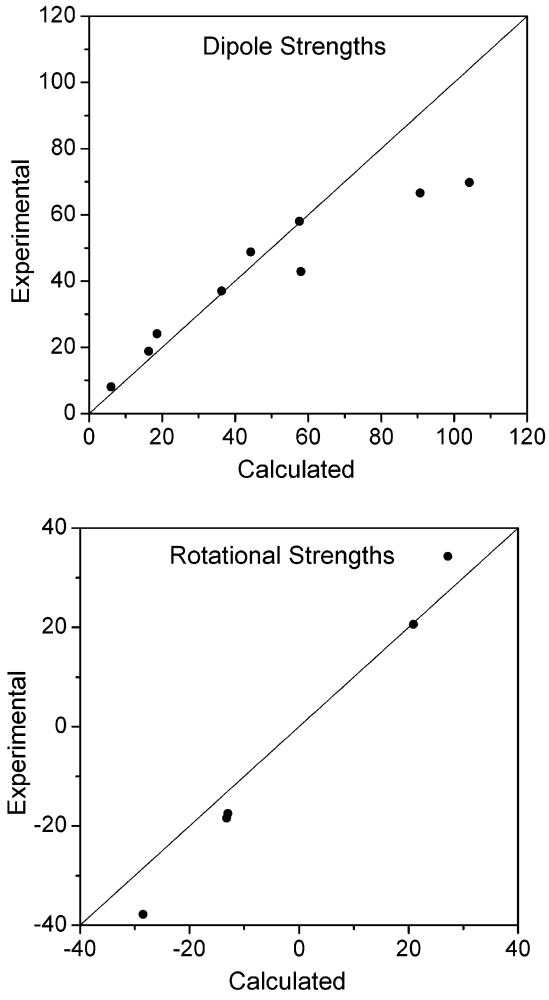

Figure 4. Plot of experimental versus predicted dipole strengths (top) and rotational strengths (bottom) for 3-chloro-1-butyne. Predicted quantities were obtained in the B3LYP/aug-cc-pVDZ calculation for the (*R*)-configuration and experimental quantities were obtained for (+)-enantiomer from integrated areas using eqs 5 and 6. The solid line has unit slope.

and predicted results from these plots. Therefore, we use PDs and RMSP differences, as defined in eqs 1 and 2. For this purpose, the frequencies, dipole strengths, and rotational strengths obtained in all calculations are compared to the corresponding experimental quantities in Table 2. The PDs and RMSP differences are summarized in Table 3. The RMSP differences for unscaled frequencies are 1, 2, and 2, respectively, in the aug-cc-pVDZ, 6-311++G(2d,2p), and aug-cc-pVTZ basis-set calculations with the B3LYP functional. The average frequencies from these three calculations also have a RMSP difference of 2. For dipole strengths, the RMSP differences are 27, 34, and 29, respectively, in the aug-cc-pVDZ, 6-311++G(2d,2p), and aug-cc-pVTZ basis-set calculations, with the average dipole strengths from these calculations giving a RMSP difference of 26. In regard to the rotational strengths, the RMSP differences are 22, 21, and 22, respectively, in the aug-cc-pVDZ, 6-311++G(2d,2p), and aug-cc-pVTZ basis-set calculations, with the average rotational strengths from these calculations giving a RMSP difference of 21. These observations indicate that the RMSP differences are rather large for the dipole and rotational strengths. Thus, when VA and VCD spectra are used to deduce the quantitative conformer populations in a multiple conformer molecule, one should expect large uncertainties in the populations determined therefrom.

To evaluate if large RMSP differences that are observed in the B3LYP calculations can be reduced by choosing another functional, calculations were repeated with the B3PW91 functional and the aug-cc-pVDZ basis set. These data are provided as Supporting Information. In regard to the dipole and rotational strengths, the RMSP differences are 36 and 34, respectively, which are larger than those obtained with the B3LYP/aug-cc-pVDZ calculation. Thus, we have not undertaken any further calculations with the B3PW91 functional.

(—)-3-Butyn-2-ol. A comparison between the experimental and B3LYP/6-31G* predicted VA and VCD spectra of (−)-3-butyn-2-ol has been reported previously,[21] with an emphasis on determining the absolute configuration. A theoretical investigation on the influence of intermolecular hydrogen bonding in (*S*)-(−)-3-butyn-2-ol was also reported.[22] However, quantitative determination of the conformer populations in (−)-3-butyn-2-ol has not been addressed previously. Three different conformations are possible for 3-butyn-2-ol, as depicted in Figure 5. These conformations are labeled as *trans*-methyl, *trans*-H, and *trans*-ethynyl, which indicate the relative orientation of the hydroxyl H atom, with respect to the methyl, C*−H, and ethynyl groups, respectively. The Gibbs energies, populations, and specific rotations that are predicted for these three conformations of the isolated molecule, using the B3LYP functional and the aug-cc-pVDZ, 6-311++G(2d,2p), and aug-cc-pVTZ basis sets, are summarized in Table 4. To evaluate the influence of solvent on these populations, the Gibbs energies were also calculated (by optimizing the geometries and performing the vibrational frequency calculations) in CCl_4 and CH_3OH solvents, using the PCM model that was implemented in the Gaussian 03 program.[20] These data are provided in the Supporting Information. The population of *trans*-ethynyl conformer in CCl_4 solvent was predicted to be 4.4%, 4.3%, and 4.7%, respectively, with the aug-cc-pVDZ, 6-311++G(2d,2p), and aug-cc-pVTZ basis sets.

TABLE 3: Percent Difference[a] between B3LYP Predicted and Experimental Frequencies (ν_i), Dipole Strengths (D_i), and Rotational Strengths (R_i) for (*R*)-(+)-3-chloro-1-butyne

band	6-31G*			aug-cc-pVDZ			6-311++G(2d,2p)			aug-cc-pVTZ			average[b]		
number	ν_i	D_i	R_i	ν_i	D_i	R_i	ν_i	D_i	R_i	ν_i	D_i	R_i	ν_i	D_i	R_i
1	5	−37		1	−26		3	−32		3	−32		2	−30	
2	5	−40		1	−23		3	−17		4	−16		3	−19	
3	4	−53		1	−13		3	−26		3	−25		2	−22	
4	4	16	−30	1	−2	−24	3	−15	−23	3	−14	−25	2	−10	−24
5	3	70	−7	0	49	1	1	43	0	1	38	1	1	43	1
6	3	67	−18	1	−9	−21	2	52	−18	2	39	−19	2	27	−19
7	2	−36	−20	1	35	−28	1	−42	−19	1	−38	−20	1	−15	−22
8	2	−5	−33	0	−2	−26	1	4	−30	1	−2	−31	1	0	−29
9	2	50		1	36		0	41		1	35		1	37	
RMSP[c]	4	46	24	1	27	22	2	34	21	2	29	22	2	26	21

[a] Percent difference is calculated as 100 x $(P_i - E_i)/E_i$, where P_i is the predicted value for band i and E_i is the corresponding experimental value, for each of the three quantities (frequency (ν_i), dipole strength (D_i), and rotational strength (R_i)). The values are rounded to whole numbers. [b] Average of the differences using aug-cc-pVDZ, 6-311++G(2d,2p), and aug-cc-pVTZ. [c] Root-mean-square percent difference, defined as RMSP = $\{\sum_{i=1}^{N}[100(P_i - E_i)/E_i]^2/N\}^{1/2}$, where P_i is the predicted value for band i, E_i the corresponding experimental value, and N the number of data points.

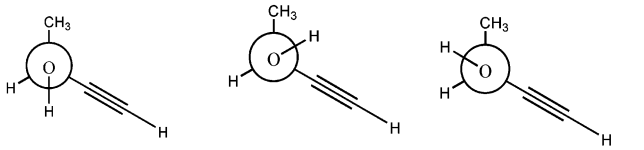

(a) Trans-methyl (b) Trans-H (c) Trans-ethynyl

Figure 5. Three conformations of 3-butyn-2-ol: (a) *trans*-methyl, (b) *trans*-H, and (c) *trans*-ethynyl.

TABLE 4: B3LYP Calculated Gibbs Energies, Populations, and Specific Rotations of Three Conformers of Isolated (*S*)-3-Butyn-2-ol

	trans-methyl	*trans*-H	*trans*-ethynyl
Gibbs Energy (in hartrees)			
aug-cc-pVDZ	−231.15361	−231.15321	−231.15070
6−311 ++G(2d,2p)	−231.20386	−231.20352	−231.20095
aug-cc-pVTZ	−231.21788	−231.21752	−231.21508
Population (%)			
aug-cc-pVDZ	58.7	38.6	2.7
6−311 ++G(2d,2p)	57.2	40.2	2.6
aug-cc-pVTZ	57.6	39.4	3.0
Specific Rotation, $[\alpha]_D$			
aug-cc-pVDZ	−110.4	28.9	64.4
6−311 ++G(2d,2p)	−88.7	29.2	84.6
aug-cc-pVTZ	−108.4	25.2	61.4

This is not significantly different from the value of ∼3% that was predicted for the isolated molecule (see Table 4). Therefore, one can conclude that, for 3-butyn-2-ol as an isolated molecule and in CCl_4 solvent, the *trans*-ethynyl conformer population is negligibly small (∼3%) and the populations of *trans*-methyl and *trans*-H conformers are significant. In CH_3OH solvent, however, the population of *trans*-ethynyl conformer is predicted to be significant (12.2%, 12.9%, and 13.2%, respectively, with the aug-cc-pVDZ, 6-311++G(2d,2p), and aug-cc-pVTZ basis sets).

The concentration dependence for both optical rotation and specific rotation is shown in Figure 6 for both CCl_4 and CH_3OH solutions. The intrinsic rotation derived from these data (Table 5) is -53.4 ± 0.1 in CCl_4 and -39.3 ± 0.3 in CH_3OH. The large difference that is observed among the intrinsic rotations in CCl_4 and CH_3OH may be attributed to the difference in conformer populations. Although the influence (besides inducing a change in conformer populations) of hydrogen bonding between CH_3OH and 3-butyn-2-ol cannot be excluded, there is no obvious way to predict such influences. Thus, we assume that the difference in intrinsic rotation of (−)-3-butyn-2-ol in CCl_4 and CH_3OH solvents results from the difference in conformer population, and we determine the conformer

TABLE 5: Intrinsic Rotation[a] ($\{\alpha\}_D$) of (−)-3-Butyn-2-ol in Different Environments

environment	$\{\alpha\}_D$
isolated molecule	-46 ± 8
carbon tetrachloride, CCl_4	-53.4 ± 0.1
methanol, CH_3OH	-39.3 ± 0.3

[a] Intrinsic rotations in CCl_4 and methanol (CH_3OH) were determined from a plot of optical rotation versus concentration (see Figure 6). For the isolated molecule, the reported value is the specific rotation that was obtained from the average of three large basis-set [aug-cc-pVDZ, 6-311++G(2d,2p) and aug-cc-pVTZ] calculations. At a given theoretical level, the predicted specific rotation of each conformer was multiplied by its population that was obtained from the Gibbs energy at the same theoretical level and summed over all three conformations.

TABLE 6: Percent Population of (*S*)-(−)-3-Butyn-2-ol Conformers (A, B, and C)[a] in Different Environments, as Deduced from Intrinsic Rotation

	CCl_4		CH_3OH	
B3LYP/basis set	A	B	A	B
aug-cc-pvdz	60	37	52	35
6311++G(2d,2p)	72	25	65	22
aug-cc-pvtz	60	37	52	35
average[b]	64 ± 7	33 ± 7	56 ± 7	31 ± 7

[a] Conformation labels are as follows: A, *trans*-methyl; B, *trans*-H; and C, *trans*-ethynyl. The population of the *trans*-ethynyl conformer (C) was assumed to be constant (at 3% in CCl_4 and 13% in CH_3OH), and the populations of *trans*-methyl conformer (A) and the *trans*-H conformer (B) were adjusted to reproduce the experimental intrinsic rotation, using the predicted specific rotation for each conformer. The sum of populations of three conformers is constrained to equal 100%. The following equation is used: $\{\alpha\}_D = X_A[\alpha]_{D,A} + (1 - X_C - X_A)[\alpha]_{D,B} + X_C[\alpha]_{D,C}$. [b] Average from three calculations.The errors reported are standard deviations.

populations in these solvents as follows. The predicted Gibbs energies for 3-butyn-2-ol in CCl_4 and CH_3OH suggest that the population of the *trans*-ethynyl conformer is ∼3% in CCl_4 and ∼13% in CH_3OH. Thus, fixing the population of *trans*-ethynyl conformer at 3% in CCl_4 and 13% in CH_3OH, the observed intrinsic rotation ($\{\alpha\}_D$) in CCl_4 and CH_3OH was fit to the populations of the remaining conformers using the equation $\{\alpha\}_D = X_A[\alpha]_{D,A} + (1 - X_C - X_A)[\alpha]_{D,B} + X_C[\alpha]_{D,C}$, where $[\alpha]_{D,C}$ is the predicted specific rotation of conformer C (*trans*-ethynyl) with a fractional population X_C. The populations that have been determined in this manner, using the specific rotations predicted in the aug-cc-pVDZ, 6-311++G(2d,2p), and aug-cc-pVTZ basis-set calculations, are summarized in Table 6. The average populations obtained in the three large basis-set

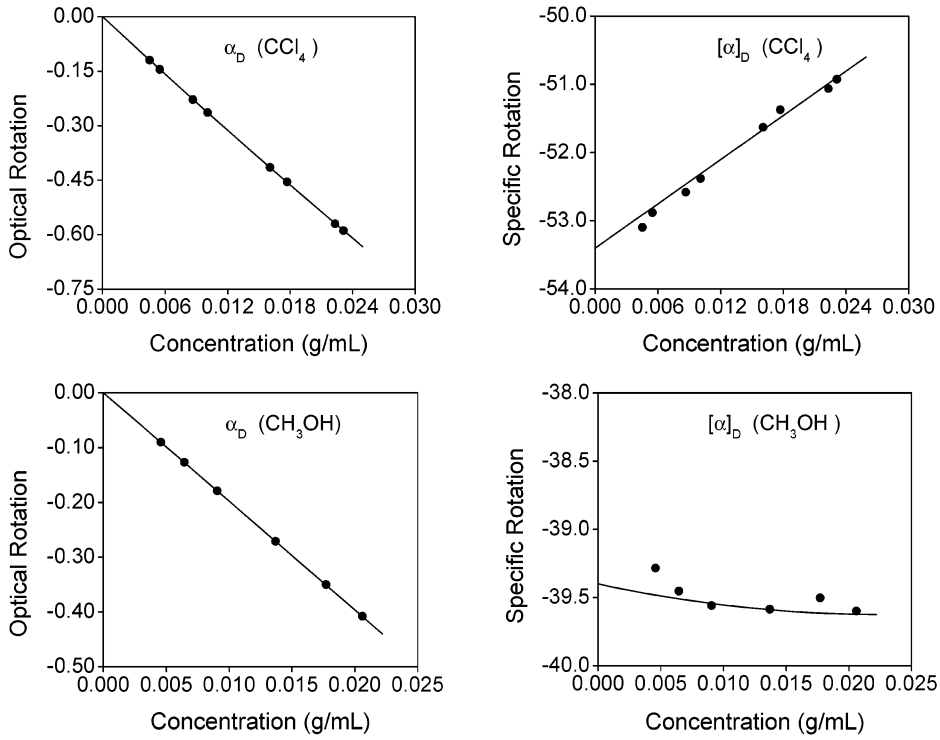

Figure 6. Optical rotation (α_D) and specific rotation ($[\alpha]_D$) of (−)-3-butyn-2-ol, as a function of concentration in CCl_4 and CH_3OH solutions. In CCl_4, a plot of α_D versus concentration was fit to $\alpha_D = 54.0c^2 - 26.7c$, and a plot of $[\alpha]_D$ versus concentration was fit to $[\alpha]_D = 108.0c - 53.4$. In CH_3OH, a plot of α_D versus concentration was fit to $\alpha_D = 218.4c^3 - 9.9c^2 - 19.7c$, and a plot of $[\alpha]_D$ versus concentration was fit to $[\alpha]_D = 436.8c^2 - 19.8c - 39.3$. Fitting of the specific rotation versus concentration required the weighted least-squares method.

calculations are as follows: 64 ± 7 for *trans*-methyl and 33 ± 7 for *trans*-H in CCl_4, 56 ± 7 for *trans*-methyl and 31 ± 7 for *trans*-H in CH_3OH. These populations represent those at infinite dilution, because intrinsic rotations are obtained at infinite dilution.

To determine the conformer populations using VA and VCD spectra, the vibrational spectral intensities are predicted for each of the three conformers of the isolated molecule using the B3LYP functional and the three large basis sets (aug-cc-pVDZ, 6-311++G(2d,2p), and aug-cc-pVTZ; see Table 7). For illustration, the simulated spectra for individual conformers obtained for (*S*)-3-butyn-2-ol in the B3LYP/aug-cc-pVDZ calculation are compared to the corresponding experimental spectra of (−)-3-butyn-2-ol in Figures 7 and 8. The predicted spectrum (which is obtained as the population-weighted sum of individual conformer spectra, using populations obtained from the Gibbs energies of the isolated molecule) is also displayed in these figures. The band numbers listed in these spectra provide correlation between the experimental bands and the corresponding theoretical bands. The qualitative "eyeballing" comparison between the simulated and observed VCD spectra clearly confirms the absolute configuration[21] of (−)-3-butyn-2-ol as (*S*). For quantitative comparison, the experimental frequencies, dipole strengths, and rotational strengths are summarized in Table 8, along with their correlation to the aug-cc-pVDZ predictions. Note that band number 4 originates from the *trans*-methyl conformer; thus, one can estimate the population of *trans*-methyl conformer from this band alone by comparing its experimental band intensity with the corresponding predicted band intensity. Thus, using the intensities predicted in the aug-cc-pVDZ calculation for band number 4, one would calculate the population of *trans*-methyl conformer to be 47% from the dipole strengths and 68% from the rotational strengths. However, a predicted population should reproduce the entire experimental spectrum quantitatively; therefore, the population that is pre-

TABLE 7: Calculated Frequencies (ν_i), Dipole Strengths (D_i), and Rotational Strengths (R_i) for Three Conformers of Isolated (*S*)-3-Butyn-2-ol at the B3LYP Level, Using Three Large Basis Sets[a]

	trans-ethynyl			*trans*-H			*trans*-methyl		
number	ν_i	D_i	R_i	ν_i	D_i	R_i	ν_i	D_i	R_i
				aug-cc-pVDZ					
1	1471	7.8	−7.7	1465	24.5	−1.1	1470	5.5	4.3
2	1462	14.2	4.1	1464	2.7	2.8	1460	13.2	−4.4
3	1395	106.8	−35.0	1396	159.7	−31.9	1398	63.4	24.9
4	1385	23.4	−1.2	1385	24.1	−3.5	1372	97.3	65.5
5	1326	17.8	−17.3	1324	33.1	17.6	1331	43.5	0.3
6	1240	177.7	53.3	1253	30.9	13.1	1271	142.2	−64.3
7	1115	310.7	−13.9	1118	223.5	−54.8	1123	141.3	−18.5
8	1089	107.0	19.6	1089	90.1	−6.0	1075	32.4	34.4
9	1033	22.2	−1.0	1030	248.7	−5.8	1041	233.0	−14.6
10	928	148.1	3.0	923	54.3	6.5	929	110.9	3.1
				6-311++G(2d,2p)					
1	1502	7.1	−7.0	1496	1.3	0.4	1502	6.2	4.0
2	1493	15.2	3.5	1495	24.0	0.7	1491	13.4	−4.2
3	1416	72.5	−18.4	1413	130.0	−37.2	1416	35.3	5.9
4	1409	37.1	−15.9	1409	45.0	7.6	1395	110.0	83.3
5	1348	16.7	−16.9	1345	29.2	14.0	1355	32.0	−2.4
6	1252	170.4	37.5	1275	33.1	9.5	1283	160.9	−61.0
7	1122	266.5	−7.2	1126	211.1	−49.0	1132	122.4	−17.9
8	1095	137.4	19.9	1089	56.3	−11.8	1088	27.0	32.6
9	1034	41.1	1.2	1035	313.9	−4.8	1033	274.2	−11.1
10	929	163.4	5.8	925	65.6	5.2	931	117.0	4.5
				aug-cc-pVTZ					
1	1497	6.0	−4.9	1491	2.3	2.0	1497	6.1	4.2
2	1488	15.0	2.9	1490	22.4	−0.8	1486	13.5	−4.4
3	1410	75.2	−13.4	1407	83.9	−35.2	1411	33.0	4.2
4	1405	42.7	−18.2	1404	90.2	6.3	1390	108.0	81.4
5	1346	16.2	−15.4	1343	29.4	13.2	1352	30.5	−3.5
6	1245	165.7	40.1	1267	32.4	10.6	1277	161.5	−59.5
7	1121	272.2	−11.1	1125	203.6	−52.3	1131	119.2	−18.4
8	1094	142.0	19.0	1088	58.7	−11.5	1086	25.7	31.7
9	1034	36.3	3.3	1033	312.0	−3.2	1032	274.2	−9.4
10	929	169.6	3.3	926	63.0	3.6	931	116.8	2.8

[a] Frequencies are given in units of cm^{-1}, dipole strengths are given in units of 10^{-40} esu^2 cm^2, and rotational strengths are given in units of 10^{-44} esu^2 cm^2.

TABLE 8: Experimental Frequencies (ν_i), Dipole Strengths (D_i), and Rotational Strengths (R_i) of (−)-3-Butyn-2-ol and Their Correlation to B3LYP Predicted Quantities for (*S*)-3-Butyn-2-ol in aug-cc-pVDZ Calculation[a]

	experimental			*trans*-ethynyl			*trans*-H			*trans*-methyl		
number	ν_i	D_i	R_i	ν_i	D_i	R_i	ν_i	D_i	R_i	ν_i	D_i	R_i
1,2	1448	32.1		1471, 1462	22.0		1465, 1464	27.2		1470, 1460	18.7	
3	1377	95.7		1395, 1385	130.2		1396, 1385	180.8		1398	63.4	
4	1356	45.8	44.8							1372	97.3	65.5
5	1327	82.5	39.2	1326	17.8	−17.3	1324	33.1	17.6	1331	43.5	0.3
6	1257	144.2	−20.0	1240	177.7	53.3	1253	30.9	13.1	1271	142.2	−64.3
7	1110	220.5	−44.2	1115	310.7	−13.9	1118	223.5	−54.8	1123	141.3	−18.5
8	1072	128.0	38.1	1089	107	19.6	1089	90.1	−6.0	1075	32.4	34.4
9	1027	258.6		1033	22.2		1030	248.7		1041	233	
10	922	101.7		928	148.1		923	54.3		929	110.9	

[a] Frequencies are given in units of cm^{-1}, dipole strengths are given in units of 10^{-40} esu^2 cm^2, and rotational strengths are given in units of 10^{-44} esu^2 cm^2.

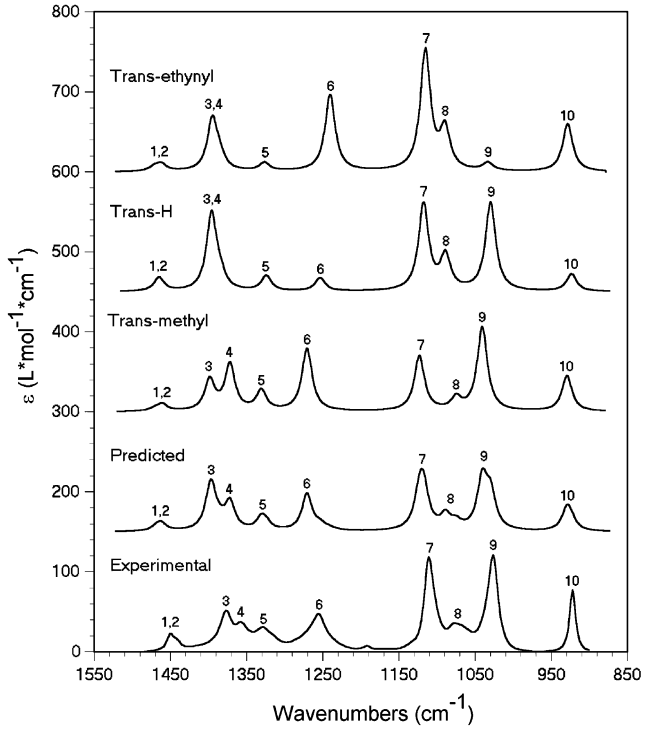

Figure 7. Comparison of experimental absorption spectra of 3-butyn-2-ol (0.103 M in CCl_4, path length of 500 μm) with the simulated absorption spectra (B3LYP/aug-cc-pVDZ; a bandwidth of 8 cm^{-1} was used in the spectral simulation) for individual conformers and with the predicted absorption spectrum (population weighted sum of conformer spectra). Populations determined from the Gibbs energies (Table 4) are used to obtain the predicted spectrum.

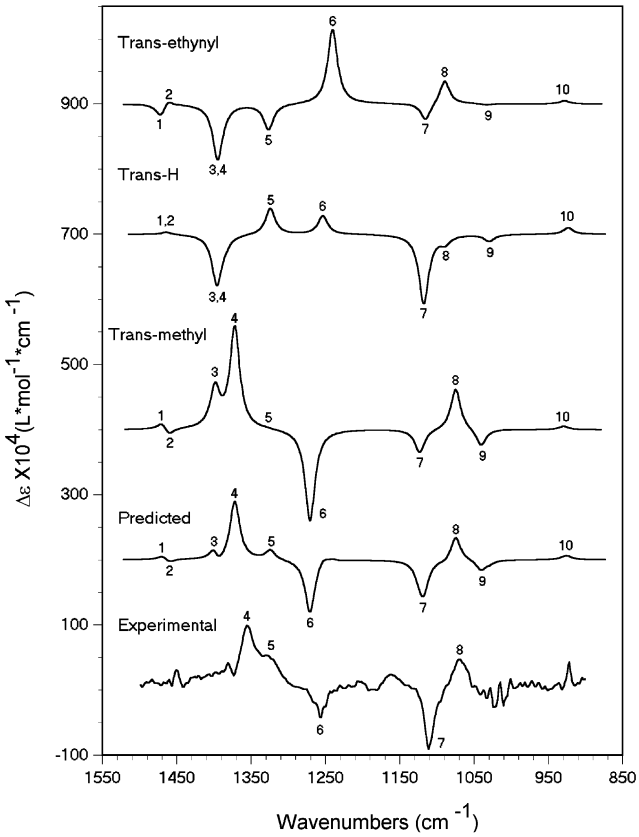

Figure 8. Comparison of experimental vibrational circular dichroism (VCD) spectra of (−)-3-butyn-2-ol (0.103 M in CCl_4, path length of 500 μm) with the simulated VCD spectra (B3LYP/aug-cc-pVDZ; a bandwidth of 8 cm^{-1} was used in the spectral simulation) for individual conformers of (*S*)-3-butyn-2-ol and with the predicted VCD spectrum (population weighted sum of conformer spectra). Populations determined from the Gibbs energies (Table 4) are used to obtain the predicted spectrum.

dicted from one band intensity would not be a true measure. For this reason, we used a regression method, utilizing eq 3 and fixing the population of *trans*-ethynyl conformer at 3%. Because the path lengths used for VA and VCD measurements are usually very small (on the order of few hundred micrometers), and low concentrations are used to avoid aggregation effects, any error in these quantities may influence the populations. Thus, a multiplicative variable (k) is introduced into the regression analysis. The equation used for regression analysis is $E_i = k[X_A P_{A,i} + (1 - X_A - 0.03)P_{B,i} + 0.03P_{C,i}]$, where conformer C is *trans*-ethynyl. The populations derived from regression analysis and associated uncertainties, at the 95% confidence level, are summarized in Table 9. Large uncertainties, as expected previously from the quantitative comparison for 3-chloro-1-butyne, are obtained here for the populations. The uncertainties in populations are slightly higher if the multiplicative variable k is not included in the regression analysis. These large uncertainties are a direct result of the discrepancies (see Figures 7 and 8) among the predicted and observed vibrational band intensities. For some bands, the experimental and predicted band intensities are similar to each other, whereas, for other bands, significant differences remain. Thus, overall quantitative agreement between the experimental and predicted VA and VCD intensities is not as good as one would like.

To evaluate the role of solvent on the predicted VA and VCD intensities, we have repeated the B3LYP calculations (using the aug-cc-pVDZ, 6-311++G(2d,2p), and aug-cc-pVTZ basis sets) of frequencies, absorption intensities, and VCD intensities using CCl_4 solvent in a PCM model. These data are provided as Supporting Information. The populations obtained from these

TABLE 9: Percent Population of *trans*-Methyl Conformer[a] of (*S*)-(−)-3-Butyn-2-ol, Deduced from Vibrational Absorption and Vibrational Circular Dichroism (VCD) Intensities

	I[b]		II[c]	
B3LYP/basis set	absorption	VCD[d]	absorption	VCD[d]
aug-cc-pVDZ	60 ± 30	55 ± 34	61 ± 27	62 ± 41
6311++G(2d,2p)	52 ± 42	51 ± 37	54 ± 40	60 ± 42
aug-cc-pVTZ	51 ± 41	52 ± 37	52 ± 40	61 ± 41
average	54 ± 37	53 ± 36	56 ± 36	61 ± 41

[a] The *trans*-ethynyl conformer population was assumed to be 3%, and sum of the populations of three conformations is constrained to equal 100%. The following equation is used for fitting: $E_i = k[X_A P_{A,i} + (1 - X_A - 0.03)P_{B,i} + 0.03P_{C,i}]$, where E_i and P_i are the respective experimental and predicted band intensities, k is a multiplicative variable, and X_A, X_B, and X_C are the respective fractional populations of the *trans*-methyl, *trans*-H, and *trans*-ethynyl conformations. [b] Determined using the predicted intensities for an isolated molecule. The average value of k obtained from the absorption intensity data in the three basis-set calculations is 1.12 (±0.27). [c] Determined using the predcited intensities in CCl_4 solvent with the PCM model. The average value of k obtained from the absorption intensity data in the three basis-set calculations is 0.88 (±0.20). [d] Band number 5 was not used in the regression. The k value obtained in the absorption fit was a fixed constant in the VCD intensity fit.

data are also included in Table 9. It is evident that the use of intensities predicted with the PCM model does not improve the errors that are estimated for the populations. We have not pursued calculations with the B3PW91 functional for 3-butyn-2-ol, because this functional did not lead to any improved results for 3-chloro-1-butyne.

In summary, for the substituted butynes studied here, the absolute configuration could be established in a straightforward manner using either intrinsic rotation or VCD intensities, in conjunction with quantum mechanical prediction of the corresponding properties. The predicted specific rotation for (+)-3-chloro-1-butyne is in excellent quantitative agreement with the observed intrinsic rotation. The predicted VA and VCD intensities for 3-chloro-1-butyne differ from the corresponding experimental quantities, with an RMSP difference of ∼20%−30%. Similar observations are noted for (−)-3-butyn-2-ol, where the errors in populations determined from intrinsic rotation of (−)-3-butyn-2-ol are not large. However, when the populations were derived from VA and VCD intensities, the error associated with the determined conformer populations is observed to be much larger. Some caution must be exercised in generalizing the success noted here for substituted butynes with specific rotation, because, for an apparently similar molecule ((−)-3-chloro-1-butene), the predicted specific rotations were reported[5] to be different from the observed specific rotations by a factor of 2.6. Thus, more investigations are needed to establish the generality of small errors noted for conformer populations that have been determined from the combined use of intrinsic rotation and specific rotation.

Conclusions

One of the smallest chiral molecules with a single conformer, (+)-3-chloro-1-butyne, has been synthesized for the first time, and its absolute configuration is determined to be (*R*), from specific rotation and vibrational circular dichroism (VCD). A quantitative comparison between the experimental and predicted vibrational band intensities in vibration absorption (VA) and VCD spectra reveal that the root-mean-square percent differences are rather large (∼30%). On the other hand, the experimental intrinsic rotation of (+)-3-chloro-1-butyne is within the uncertainties associated with specific rotation that has been predicted by large basis sets using the B3LYP functional. Similar studies, using specific rotation, VA, and VCD on a related molecule ((−)-3-butyn-2-ol), with three different conformers, indicate that the absolute configuration of this molecule is (*S*). The population of *trans*-methyl conformer, as determined from the observed intrinsic rotation in CCl_4 and the predicted specific rotations using large basis sets with the B3LYP functional, is 64% ± 7%. The analogous population that has been determined from VA and VCD intensities is similar to that determined from intrinsic rotation; however, the uncertainty in the deduced population is substantially larger.

Acknowledgment. The authors thank Dr. Kenneth Ruud, for providing a developmental version of the DALTON program, which was used to calculate the specific rotations reported here; Dr. David Wright, for allowing us to use the electronic circular dichroism (ECD) spectrometer; and Dr. Ned Porter, for allowing us to use chiral GC column. This material is based upon work that has been supported by the National Science Foundation (under Grant No. 0092922). Any opinions, findings, and conclusions or recommendations expressed in this material are those of the author(s) and do not necessarily reflect the views of the National Science Foundation.

Supporting Information Available: ECD spectrum of (+)-3-chloro-1-butyne, B3PW91/aug-cc-pVDZ results for (*R*)-3-chloro-1-butyne, PCM model results for (*S*)-3-butyn-2-ol (PDF). This material is available free of charge via the Internet at http://pubs.acs.org.

References and Notes

(1) Parr, R. G.; Yang, W. *Density Functional Theory of Atoms and Molecules*; Oxford University Press: Oxford, U.K., 1989.

(2) (a) Wang, F.; Wang, Y.; Polavarapu, P. L.; Li, T.; Drabowicz, J.; Pietrusiewicz, K. M.; Zygo, K. *J. Org. Chem.* **2002**, *67*, 6539−6541. (b) Freedman, T. B.; Dukor, R. K.; van Hoof, P. J. C. M.; Kellenbach, E. R.; Nafie, L. A. *Helv. Chim. Acta* **2002**, *85*, 1160−1165. (c) Devlin, F. J.; Stephens, P. J.; Osterle, C.; Wiberg, K. B.; Cheeseman, J. R.; Frisch, M. J. *J. Org. Chem.* **2002**, *67*, 8090−8096. (d) Ashvar, C. S.; Stephens, P. J.; Eggimann, T.; Wieser, H. *Tetrahedron: Asymmetry* **1998**, *9*, 1107.

(3) Devlin, F. J.; Stephens, P. J. *J. Am. Chem. Soc.* **1999**, *121*, 7413−7414.

(4) Wang, F.; Polavarapu, P. L. *J. Phys. Chem. A* **2000**, *104*, 6189−6196.

(5) Wiberg, K. B.; Vaccaro, P. H.; Cheeseman, J. R. *J. Am. Chem. Soc.* **2003**, *125*, 1888−1896.

(6) Polavarapu, P. L.; Petrovic, A.; Wang, F. *Chirality* **2003**, *15*, S143−S149; *15*, 801.

(7) Polavarapu, P. L. *Mol. Phys.* **1997**, *91*, 551−554.

(8) (a) Ruud, K.; Helgaker, T. *Chem. Phys. Lett.* **2002**, *352*, 533−539. (b) Yabana, K.; Bertsch, G. F. *Phys. Rev. A* **1999**, *60*, 1271−1279. (c) Cheeseman, J. R.; Frisch, M. J.; Devlin, F. J.; Stephens, P. J. *J. Phys. Chem. A* **2000**, *104*, 1039−1046. (d) Autschbach, J.; Patchkovskii, S.; Ziegler, T.; van Gisbergen, S. J. A.; Baerends, E. J. *J. Chem. Phys.* **2002**, *117*, 581−592. (e) Grimme, S.; Furche, F.; Ahlrichs, R. *Chem. Phys. Lett.* **2002**, *361*, 321−328.

(9) For a review, see: Polavarapu, P. L. *Chirality* **2002**, *14*, 768−781; **2003**, *15*, 284−285.

(10) (a) Miller, T.; Wiberg, K. B.; Vaccaro, P. H. *J. Phys. Chem. A* **2000**, *104*, 5959−5968. (b) Miller, T.; Wiberg, K. B.; Vaccaro, P. H.; Cheeseman, J. R.; Frisch, M. J. *J. Opt. Soc. Am. B* **2002**, *19*, 125−141.

(11) (a) Munyemana, F.; Frisque-Hesbian, A. M.; Devos, A.; Ghosez, L. *Tetrahedron Lett.* **1989**, *30*, 3077−3080. (b) Brandsma, L.; Verkruijsse, H. D. *Synthesis of Acetylenes, Allenes and Cumulenes, A Laboratory Manual*; Elsevier: New York, 1981; p 217.

(12) Curme, H. G.; Heller, W. Optical Rotation−Experimental Techniques and Physical Optics. In *Polarimetry*; Weissberger, A., Rossiter, B. W., Eds.; Techniques of Chemistry, Vol. I. Physical Methods of Chemistry. Part IIIc; Wiley−Interscience: New York, 1972; pp 51−182.

(13) Cheeseman, J. R.; Frisch, M. J.; Devlin, F. J.; Stephens, P. J. *Chem. Phys. Lett.* **1996**, *252*, 211−220.

(14) PeakFit Program, Version 4.1.1, SPSS, Inc., Chicago, IL.
(15) Faulkner, T. R. Ph.D. Thesis, University of Minnesota, Minneapolis, MN, 1976.
(16) DataFit for Windows, Version 7.1, Oakdale Engineering, Oakdale, PA.
(17) Helgaker, T.; Jensen, H. J. Aa.; Joergensen, P.; Olsen, J.; Ruud, K.; Aagren, H.; Auer, A. A.; Bak, K. L.; Bakken, V.; Christiansen, O.; Coriani, S.; Dahle, P.; Dalskov, E. K.; Enevoldsen, T.; Fernandez, B.; Haettig, C.; Hald, K.; Halkier, A.; Heiberg, H.; Hettema, H.; Jonsson, D.; Kirpekar, S.; Kobayashi, R.; Koch, H.; Mikkelsen, K. V.; Norman, P.; Packer, M. J.; Pedersen, T. B.; Ruden, T. A.; Sanchez, A.; Saue, T.; Sauer, S. P. A.; Schimmelpfennig, B.; Sylvester-Hvid, K. O.; Taylor, P. R.; Vahtras, O. *Dalton, A Molecular Electronic Structure Program*; University of Oslo: Oslo, Norway, 2001.
(18) Available on the Internet at www.emsl.pnl.gov:2080/forms.
(19) Helgaker, T.; Ruud, K.; Bak, K. L.; Jorgensen, P. *Faraday Discuss.* **1994**, *99*, 165−180.
(20) Frisch, M. J.; Trucks, G. W.; Schlegel, H. B.; Scuseria, G. E.; Robb, M. A.; Cheeseman, J. R.; Zakrzewski, V. G.; Montgomery, J. A., Jr.; Stratmann, R. E.; Burant, J. C.; Dapprich, S.; Millam, J. M.; Daniels, A. D.; Kudin, K. N.; Strain, M. C.; Farkas, O.; Tomasi, J.; Barone, V.; Cossi, M.; Cammi, R.; Mennucci, B.; Pomelli, C.; Adamo, C.; Clifford, S.; Ochterski, J.; Petersson, G. A.; Ayala, P. Y.; Cui, Q.; Morokuma, K.; Malick, D. K.; Rabuck, A. D.; Raghavachari, K.; Foresman, J. B.; Cioslowski, J.; Ortiz, J. V.; Stefanov, B. B.; Liu, G.; Liashenko, A.; Piskorz, P.; Komaromi, I.; Gomperts, R.; Martin, R. L.; Fox, D. J.; Keith, T.; Al-Laham, M. A.; Peng, C. Y.; Nanayakkara, A.; Gonzalez, C.; Challacombe, M.; Gill, P. M. W.; Johnson, B. G.; Chen, W.; Wong, M. W.; Andres, J. L.; Head-Gordon, M.; Replogle, E. S.; Pople, J. A. *Gaussian 98/03*, Gaussian, Inc.: Pittsburgh, PA.
(21) Wang, F.; Polavarapu, P. L. *J. Phys. Chem. A* **2000**, *104*, 1822−1826.
(22) Cappelli, C.; Corni, S.; Mennucci, B.; Cammi, R.; Tomasi, J. *J. Phys. Chem. A* **2002**, *106*, 12331−12339.